Astron. Astrophys. 349, 203–208 (1999)

ASTRONOMY AND ASTROPHYSICS

Multiple shells in the circumstellar envelope of IRC+10216⋆

N. Mauron[1] **and P.J. Huggins**[2]

[1] Groupe d'Astrophysique, CNRS and Université de Montpellier, Case 072, Place Bataillon, F-34095 Montpellier Cedex 05, France (mauron@merlin.graal.univ-montp2.fr)
[2] Physics Department, New York University, 4 Washington Place, New York, NY 10003, USA

Received 28 April 1999 / Accepted 14 June 1999

Abstract. We report deep B and V-band images of IRC+10216 which reveal its extended circumstellar envelope in dust scattered, ambient Galactic light. The envelope is detected out to $\sim 200''$ from the central star and its structure records the mass-loss history over the past $\sim$ 8,000 yr. The envelope is roughly spherically symmetric but is composed of a series of discrete, incomplete, concentric shells. The shells are thin ($\sim 1''$–$2''$) and separated by $\sim 5''$–$20''$, which corresponds to $\sim$ 200–800 yr. The shells suggest that some process modulates the mass-loss of the star on this time scale. The presence of shells also means that models of the extended envelope which have been based on smooth distributions of the circumstellar material need to be re-examined.

Key words: stars: AGB and post-AGB – stars: mass-loss – stars: individual: IRC+10216 – stars: circumstellar matter

1. Introduction

IRC+10216 (CW Leo) is the nearest carbon star with a thick circumstellar envelope. It is not visible on the blue plate of the Palomar Sky Survey because of extinction by circumstellar dust, but at longer wavelengths it rapidly becomes brighter than any other evolved star. The strength of the infrared and millimeter spectrum of IRC+10216 means that it has been intensively observed, and it ranks as one of the most important cases for the study of mass-loss on the Asymptotic Giant Branch (see, e.g., the review by Olofsson 1996).

Many properties of IRC+10216 are well established from observations. The terminal expansion velocity of the gas is 14 km s^{-1}, the mass-loss rate is $\sim 2 \times 10^{-5}$ M$_\odot$ yr^{-1}, and the envelope can be traced out to $\sim 200''$ from the star in CO (see, e.g., Huggins 1995). For the distance we adopt the value of 120 pc given by Loup et al. (1993) which is consistent with most recent estimates. Nearly 50 molecular species have been detected in the envelope, and it serves as the best example of carbon-rich circumstellar chemistry (e.g., Glassgold 1996).

One important aspect of IRC+10216 that is not well described by observations is the small scale structure of the envelope. This is relevant for directly probing the geometry of the mass-loss process, and for the construction of detailed models. There is a long history of high angular resolution observations of the very central regions of IRC+10216 where the radiation field is strongest. Recent examples in the near infrared at sub arc-second resolution include Weigelt et al. (1998), Haniff & Buscher (1998), and Skinner et al. (1998). These reveal a complex region where the radiation from the star filters out through intricate, inner layers of the envelope. Other studies have broadened the area over which structure can be seen, especially molecular line imaging with millimeter interferometers (Lucas & Guélin 1999, and references therein).

In spite of its faintness at short wavelengths, the most extended view of IRC+10216 with arc-second resolution is a deep V-band image obtained more than a decade ago by Crabtree et al. (1987). This image shows a small core due to scattered light from the central star, surrounded by an extended halo which Martin & Rogers (1987) interpret as the dust envelope seen in scattered, ambient, Galactic light. The envelope is detected out to $\sim 40''$ from the star and shows previously unseen structure in the form of distinct arcs.

In this paper we extend this approach to study the global structure of the circumstellar envelope of IRC+10216. We present new B and V-band images which go significantly deeper than the earlier work. The images show the dust envelope illuminated by Galactic light extending out to $\sim 200''$ from the star, and they reveal a multiple shell structure. Some implications of this structure are discussed.

2. Observations

The observations were carried out in 1998, February 17–18, with the Canada-France-Hawaii Telescope (CFHT) by D. Crabtree. Two 20 minute exposures in the B-band and four in the V-band were obtained with the MOS focal reducer installed at the Cassegrain focus. The detector was an STIS2 2048×2048 21 μ-pixel CCD array, with read-out noise 0.7 ADU and gain 4.52 e ADU^{-1}. The image scale was found to be 0.436±0.002 arc-

Send offprint requests to: N. Mauron

⋆ Based on observations made with the Canada France Hawaii Telescope, operated by CNRS, the National Research Center of Canada, and the University of Hawaii, and partly at the Haute Provence Observatory (CNRS).

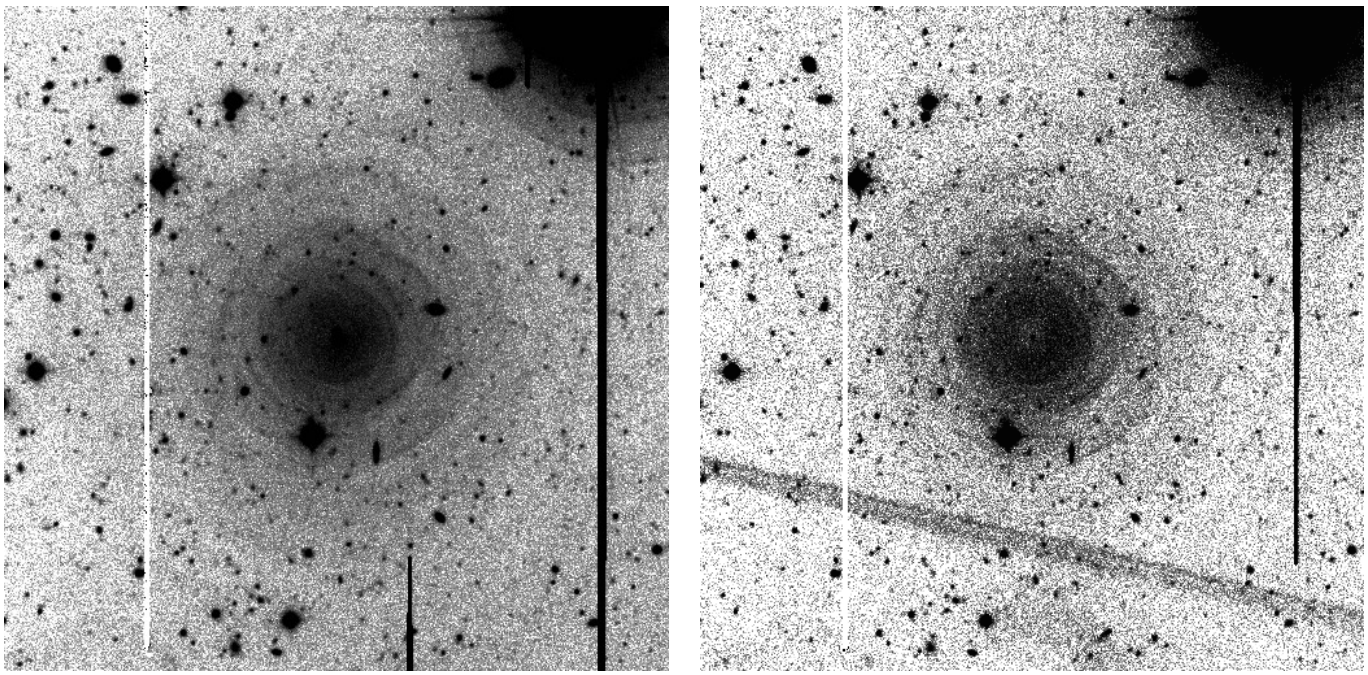

Fig. 1. V (left panel) and B (right panel) images of IRC+10216. The field is $223'' \times 223''$. North is at the top, East to the left.

Table 1. Observations of IRC+10216

Band	Exposures (min)	Frame #	Sky level (ADU $\pm\sigma$)	Halo peak (ADU)	Halo surface brightness (OHP) (mag arcsec^{-2})	(W m^{-2} Hz^{-1} sr^{-1})
V	4×20	430256o–59o	2743 $\pm$14	140	25.1	14×10^{-23}
B	2×20	430260o–61o	917 $\pm$11	48	25.8	8×10^{-23}

sec pixel^{-1}. Because of vignetting, only the central 1200×1200 pixel field was usable, representing about $8.7' \times 8.7'$. Biases, dome and sky flats were obtained, but no photometric calibration on standard fields was secured. However, additional observations of IRC+10216 were obtained using the 1.2 m telescope of the Observatiore de Haute Provence (OHP), and they provide photometric calibration of the images. Details of these observations will be given elsewhere.

The CFHT images were cleared of cosmic ray events, and the different frames were stacked to obtain B and V images with low noise levels. It was found necessary to further flatten the summed images with a 2nd order polynomial function which was adjusted on the edges of the fields and iteratively optimized.

The final B and V-band images of IRC+10216 are shown in Fig. 1. The field is $223'' \times 223''$, with IRC+10216 at the center. The B image is somewhat lower in signal-to-noise than V and has an obvious blemish, but this is only cosmetic. The prominent feature in the top right of the field is an $R = 10.6$ mag star. The object $35''$ South of the center is a $V = 16.0$ mag star, and the object $34''$ West of the center is an $R = 19.8$ mag background galaxy. Because of the depth of the image, many galaxies are also seen at low levels, especially to the East of the center, which is possibly the location of a cluster. The sky levels and other details of the images are given in Table 1.

3. Results and discussion

3.1. The B and V-band images

The new images of IRC+10216 (Fig. 1) are deeper than the earlier V-band image reported by Crabtree et al. (1987) and show more detail of the extended envelope than previously available. The two images are similar in appearance. Both show a small, central core of scattered light from the central star, fainter in B as expected from the red color of the star and the larger opacity of the envelope at shorter wavelengths. Both images clearly show an extended, roughly circularly symmetric halo. A striking feature is the appearance of multiple shell-like structures.

3.2. Averaged radial profiles and extent of the envelope

In order to characterize the overall distribution of the envelope we have obtained radial intensity profiles, averaged in azimuth. Several thousand background galaxies and field stars were located by hand or DAOPHOT and masked out, along with large halos around bright stars and several optical ghosts and defects. The mean intensity was then determined in a series of annuli $4''$ thick, centered on the star. The number of pixels averaged in each annulus ranges from $\sim$100 (near the star) to several thousand (farther out). Because the net flux from the envelope is

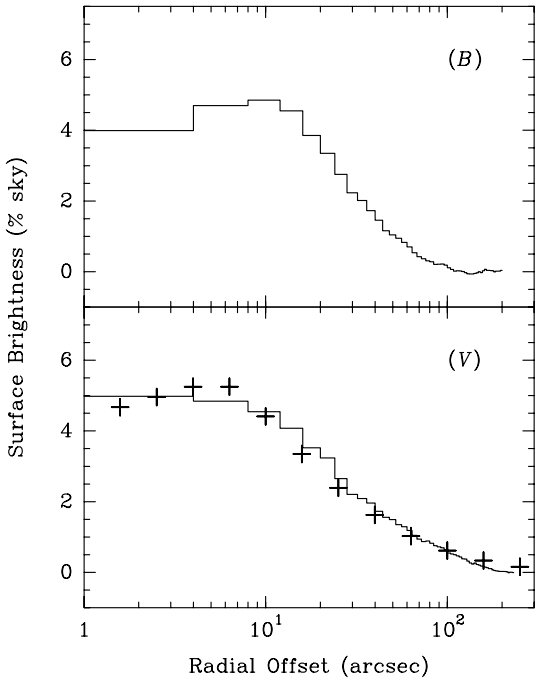

Fig. 2. Azimuthally averaged radial profiles of IRC+10216 in B (upper panel) and V (lower panel), normalized relative to the sky background. The V-band profile is restricted to data in the sector PA=0°–120° which was found to be clearest of contamination. A model V-band profile based on dust scattered Galactic light (Martin & Rogers 1987) is shown by crosses in the lower panel.

small relative to the sky flux ($\lesssim 6\%$), we took care that the rms value for each annulus was statistically the same for all annuli.

The radial intensity profiles are shown in Fig. 2, relative to the sky. The limitation on the measurements is variation in the background, and for the V-band data we restrict the measurements to a sector within PA=0°–120°, where the background is clearest of contamination. The profiles exhibit a distinct plateau within $\sim 15''$ of the star, and we give the photometric calibration of this level from the OHP observations in the last two columns of Table 1.

The envelope can be directly seen in the images out to $\sim 80''$ from the star, but in the averaged profiles it can be detected considerably farther out, in the clearest sectors to $\sim 200''$. There is no sign of an edge to the envelope, and the extent measured is limited by the sensitivity. From the distance to IRC+10216 and the expansion velocity of the envelope, $200''$ corresponds to matter ejected from the star $\sim 8,000$ yr ago.

3.3. Illumination of the envelope

The general shape of the B and V intensity profiles confirms that the images of the extended envelope are seen in scattered ambient Galactic light. For a centrally illuminated envelope, the observed intensity is a steep function of the radial offset, and this corresponds to the diffuse stellar images seen in the central few arc seconds. The extended profiles are, however, roughly flat in the plateau region, and fall off roughly as $\sim r^{-1}$ farther out. These two regions correspond to where the optical depth is $\gtrsim 1$ and $\lesssim 1$, respectively, for *external* radiation. In this case, the optically thin $\sim r^{-1}$ dependence can be simply understood in terms of the line of sight column density through the envelope.

A model for the dust scattering of ambient Galactic light by the envelope of IRC+10216 has been described by Martin & Rogers (1987). Their model includes a detailed treatment of the dust particles, and assumes a constant mass loss rate with an r^{-2} density profile. In Fig. 2 we compare the observed intensity profile with the model profile in V, scaled to give a reasonable overall fit. In fact the peak surface brightness of the model plateau region (10^{-22} W m^{-2} Hz^{-1} sr^{-1}) is close to our photometric calibration made with the OHP observations (Table 1).

The dust scattering model provides a good description of the average V-band intensity profile (Fig. 2). The model with external illumination only does predict a small dip towards the center which is not seen in the V-band profile, but it is likely that our measurements in the inner annulus are slightly affected by the light from the central star. The dip is expected to be more prominent in B (although Martin & Rogers give no detailed calculations for this band), and in fact this is observed to be the case: a distinct dip is seen in the observed B profile within $\sim 10''$ of the center (Fig. 2), and even directly in the B image in Fig. 1.

3.4. Properties of the shells

The most striking aspect of our observations of IRC+10216 is the appearance of distinct, multiple shells in the envelope. In order to show these fully, we have combined the B and V images and replaced the background stars and galaxies with local averages. The composite image in a field of $131'' \times 131''$ is shown in Fig. 3 in two different formats: the direct image, and one in which the average radial profile has been subtracted, to bring out the details. A few patches in the images are residue of the removal of the brightest background objects, and these should be ignored.

Several properties of the shells are readily apparent from the data. First, the system of shells overall shows rough circular symmetry. Thus the mass-loss *on average* is roughly isotropic, and from the comparison of the dust scattering model with the data in the previous section, the mass loss has *on average* been relatively constant over time for several thousand years. These are consistent with other measurements of the extended envelope in both dust and gas (e.g., Tamura et al. 1988, Huggins et al. 1988, Truong-Bach et al. 1991).

On smaller scales the picture is quite different. Although the individual shells appear as roughly circular arcs, they are incomplete, typically covering $\sim 30°$–$90°$ in azimuth with respect to the central star, and in some cases they deviate perceptibly from circular. Moving away from the star, the intensity is seen to drop across the arcs, which shows they are indeed the edges of shells, rather than filaments. The shells are evidently thin, with very sharp outer edges.

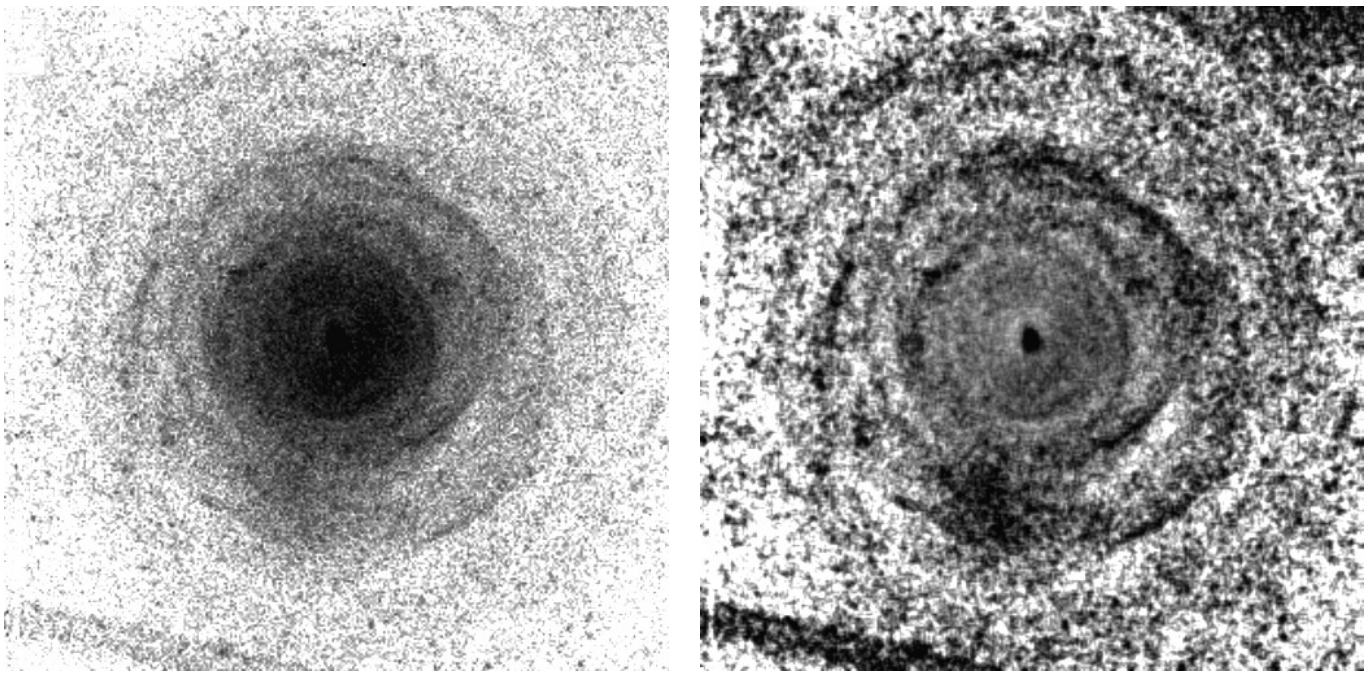

Fig. 3. Composite $B+V$ image of IRC+10216, shown with a regular transfer function (left) and with an average radial profile subtracted (right) to enhance the contrast. The field is $131'' \times 131''$. North is at the top, East to the left.

Some of these features can be better seen in Fig. 4 where we plot representative radial strips (20° wide) through the shells. The uncertainty in the intensities is small (3–5%) so most of the structure seen is real. The two plots at the top of Fig. 4 are adjacent strips (to the NW) and it can be seen that they exhibit quite similar, though not identical, features. The next two strips point to the NE and SW in opposite directions and have essentially no correlated features. The structure in the strip at P.A.=214° shows a particularly clear shell profile: from 30″ to 42″ the intensity is nearly constant, it then rises to a limb brightened peak, and falls abruptly to the outside by a factor of nearly two in $\lesssim 2''$. Note that when all sectors are averaged, the shells are not seen.

The spacing of the shells does not obviously show a regular spatial pattern, but the typical radial separation is $\sim 5''$–$20''$ which corresponds to a time interval of 200–800 yr. From consideration of a simple model of limb brightened shells, as in Mauron (1997) but modified for external, optically thin illumination, the density contrast between the shells and intershell regions is inferred to be quite large, up to a factor of 10.

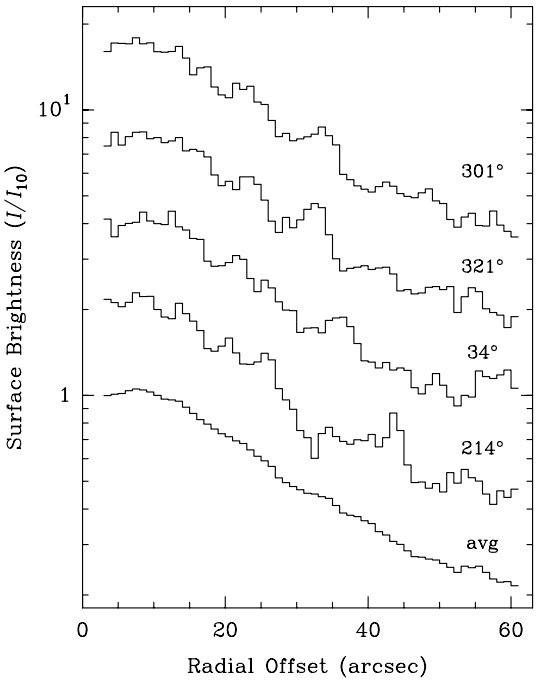

Fig. 4. Radial strips through the shells of IRC+10216 in the composite $B+V$ image. The strips are 20° wide and are labeled by PA. The strip labeled avg is the average over 360° in azimuth for reference. Intensities are relative to the value at $10''$, scaled by factors of 2 from bottom to top. The uncertainties in the intensities of the 20° sectors are 3–5%.

3.5. Relation of the dust shells to the gas

The relation of the dust shells to the distribution of gas in the envelope is of interest because in AGB envelopes the dust and gas are not completely coupled. The dust is expected to drift through the gas, in the case of IRC+10216, at a speed of $\sim$ 2 km s^{-1} (Kwan & Hill 1977). In a homogeneous envelope, this relative motion has no major effect on the structure, but in a multiple shell envelope, this might not be the case.

The gas distribution in IRC+10216 is not known in detail on the size scales of interest, but useful information is available

from interferometer maps of the envelope in millimeter emission lines of rare molecules. In the best cases the resolution is $\sim 3''$. Lucas & Guélin (1999) have summarized these observations of IRC+10216 and give an inventory of the emission peaks of a number of species in the envelope. The peaks from different species often coincide, which suggests they trace out local density enhancements in the gas, and their distribution suggest rings. In Fig. 5 we superpose the distribution of these molecular clumps seen in representative species CN, HNC, and HC_3N on the dust shell image.

Although most of the millimeter data are at offsets $\lesssim 20''$, inside the region where our dust shells are most clearly defined, there does seem to be a relation between the two sets of data. The main molecular ring corresponds to the rims of the most prominent, inner dust shells, and the clearly separated double molecular ring to the NW matches a similar structure in the dust. We tentatively conclude that the dust shells and the gas clumps are roughly co-spatial, but this needs to be explored further. One promising direction is the recent detection of narrow, millimeter CO components in the extended envelope which vary in strength and velocity with position (Groenewegen & Ludwig 1998). It is probable that these components are the gas counterparts of the dust shells we observe, and this can be checked when they are more fully mapped.

As an important archetype for the study of AGB stars, the envelope of IRC+10216 has been the focus of numerous theoretical models of the dust and gas. Although it is recognized that the mass-loss process itself in AGB stars is time dependent (e.g., Fleischer et al. 1992; Feuchtinger et al. 1993), the typical assumption in modeling the extended envelope of IRC+10216 is that the matter is homogeneous. This may be adequate for some purposes, but for others the presence of the shells will need to be considered. One example is the thermal model of the envelope of Kwan & Hill (1977) and its many later refinements, where variations due to the shells will affect both the dust-gas heating, and the radiative transfer of important cooling lines such as those of CO. A second example is the photo-chemical model which describes the effects of ambient UV photons on the chemical structure of the envelope (e.g., Glassgold 1996). The presence of physical shells will affect the penetration of dissociating radiation into the envelope, and will localize the emission of various species in the rings, which is already a characteristic of the observations noted above.

3.6. Origin of the shells

IRC+10216 is the only AGB star where many nested shells have been seen in the envelope, but the identification of similar shells around other AGB stars is extremely difficult. There is, however, spectroscopic evidence for episodic mass-loss in AGB envelopes (e.g., Bernat 1981; Ridgway 1981), and multiple shells have been directly imaged around a number of post-AGB objects and planetary nebulae, where the remnant AGB envelope is illuminated by the central star, e.g., CRL 2688 (Crabtree & Rogers 1993, Sahai et al. 1998), and IRAS 17150-3224 (Kwok et al. 1998). The presence of multiple shells in some of the best studied objects, and the striking similarity of the shells in IRC+10216 and CRL 2688, suggests that shells are common, and that IRC+10216 might be typical of late AGB stars.

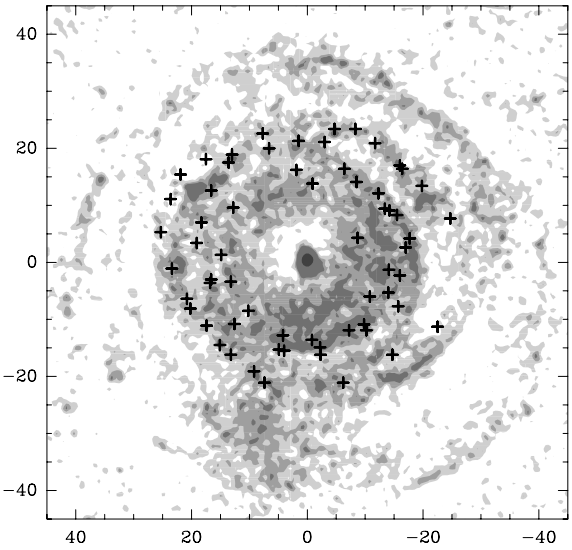

Fig. 5. Comparison of the dust and gas shells in IRC+10216. The crosses show the location of emission peaks in the molecules CN, HNC, and HC_3N (Lucas & Guélin 1999), superposed on a filled contour version of Fig. 3. The axes are labeled in arcseconds from the center.

The geometry of the shells places important constraints on their origin, as discussed for CRL 2268 by Sahai et al. (1998). In IRC+10216 these constraints include the irregular timescale of the shell spacing (200–800 yr), the different directions and limited solid angle of each shell, and their rough isotropy when averaged over time. An additional factor is the thin, bubble-like structure seen, although this may be partly the result of their development, rather than their initial formation.

The long time interval for thermal pulses (10^4–10^5 yr), rules them out as the formation mechanism for the shells, although they are good candidates for the remarkable single shells seen in a few AGB envelopes (Olofsson et al. 1990; Olofsson et al. 1996; Schröder et al. 1998).

A model in which shells are produced by binary modulation of the mass-loss has been proposed by Harpaz et al. (1997) for CRL 2688, and could in principle apply to IRC+10216 as well. Such a model does not readily fit in with the somewhat irregular distribution of arcs that we observe, and is not favored by Sahai et al. (1998) for CRL 2688 for similar reasons. However, in the context of a binary model, it is interesting that Guélin et al. (1993) earlier pointed out that IRC+10216 is not centered in molecular maps of MgNC, C_4H, and other carbon molecules, but is offset by $\sim 2''$ to the West. They suggested that this may be caused by the relative motion of the star and the envelope, caused by a binary companion. This offset is also clearly seen in the corresponding part of our dust shell image (Figs. 3 and 5). However, the structure of the shells farther out does not show a clear systematic pattern, and the asymmetry may just reflect the irregular nature of the shell ejections.

Alternative explanations may lie in some episodic process intrinsic to the star which affects the mass-loss. Layered, shell-like gas and dust distributions have been obtained in time-dependent model winds (e.g., Winters et al. 1998), but the corresponding timescales are only a few pulsation periods, i.e. $\sim$ 5–10 yr, which is too short to explain the observed shells. The behavior of stars on longer, relevant timescales is essentially unexplored, so it is not possible to come to firm conclusions on this here. It is interesting to note that similar timescales (200–1000 yr) are seen for the shells in IRC+10216, CRL 2688, and IRAS 17150-3224, and in the M supergiant μ Cep, where shells are seen in K I emission (Mauron 1997). This may reflect some general property of cool, luminous stars.

4. Conclusions

The observations reported here reveal the extended envelope of IRC+10216 in dust scattered ambient Galactic light. The envelope is detected out to $\sim 200''$ from the central star, and is seen to have a complex, multiple shell structure. The shells are thin and incomplete, with a typical separation $\sim 5''$–$20''$ which corresponds to $\sim$ 200–800 yr.

This shell structure is probably typical of many AGB stars, and raises interesting questions concerning the origin of the shells, and their development as the envelope expands. As an important archetype for the study of AGB stars, the presence of the shells also means that detailed models of the envelope which have been based on smooth distributions of material may need to be re-examined.

Acknowledgements. The authors are grateful to the directors of the CFHT for discretionary time, and to D. Crabtree for obtaining the images. They also thank the referee, J.M. Winters, for useful remarks. This work is supported in part by the Groupes de Recherche of the Centre National de Recherche Scientifique "Physico-chimie du Milieu Insterstellaire" and "Milieux Circumstellaires", and by NSF grant AST-9617941.

References

Bernat A.P., 1981, ApJ 246, 184
Crabtree D.R., Rogers C., 1993, In: Schwarz H. (ed.) Mass Loss on the AGB and Beyond. ESO, Garching, p. 255
Crabtree D.R., McLaren R.A., Christian C.A., 1987, In: Kwok S., Pottasch S.P. (eds.) Late stages of stellar evolution. Reidel, Dordrecht, p. 145
Fleischer A.J., Gauger A., Sedlmayr E., 1992, A&A 266, 321
Feuchtinger M.U., Dorfi E.A., Höfner S., 1993, A&A 273, 513
Glassgold A.E., 1996, ARA&A 34, 241
Groenewegen M.A.T., Ludwig H.-G., 1998, A&A 339, 489
Guélin M., Lucas R., Cernicharo J., 1993, A&A 280, L19
Haniff C.A., Buscher D.F., 1998, A&A 334, L5
Harpaz A., Rappaport S., Soker N., 1997, ApJ 487, 809
Huggins P.J., 1995, Ap&SS 224, 281
Huggins P.J., Olofsson H., Johansson L.E.B., 1988, ApJ 332, 1009
Kwan J., Hill F., 1977, ApJ 215, 781
Kwok S., Su K.Y.L., Hrivnak B.J., 1998, ApJ 501, L117
Loup C., Forveille T., Omont A., Paul J.F., 1993, A&AS 99, 291
Lucas R., Guélin M., 1999, In: Le Bertre T., Lèbre A., Walkens C., IAU Symp. 191, Assymptotic Giant Branch Stars. In press
Martin P.G., Rogers C., 1987, ApJ 322, 374
Mauron N., 1997, A&A 326, 300
Olofsson H., 1996, Ap&SS 245, 169
Olofsson H., Carlstrom U., Eriksson K., et al., 1990, A&A 230, L13
Olofsson H., Bergman P., Eriksson K., et al., 1996, A&A 311, 587
Ridgway S.T., 1981, In: Iben Jr. I., Renzini A. (eds.) Physical Process in Red Giants. Reidel, Dordrecht, p. 305
Sahai R., Trauger J.T., Watson A.M., et al., 1998, ApJ 493, 301
Skinner C.J., Meixner M., Bobrowsky M., 1998, MNRAS 300, L29
Schröder K.-P., Winters J.M., Arndt T.U., Sedlmayr E., 1998, A&A 335, L9
Tamura M., Hasegawa T., Ukita N., et al., 1988, ApJ 326, L17
Truong-Bach, Morris D., Nguyen-Q-Rieu, 1991, A&A 249, 435
Weigelt G., Balega Y., Bloecker T., et al., 1998, A&A 333, L51
Winters J.M., 1998, Ap&SS 255, 257